# *NAUTILUS-DTU10* MW Floating Offshore Wind Turbine at Gulf of Maine: Public numerical models of an actively ballasted semisubmersible

IOP Conf. Series: Journal of Physics: Conf. Series **1102** (2018) 012015 doi:10.1088/1742-6596/1102/1/012015

# *NAUTILUS-DTU10* MW Floating Offshore Wind Turbine at Gulf of Maine: Public numerical models of an actively ballasted semisubmersible

**J Galván[1], M J Sánchez-Lara[1,2], I Mendikoa[1], G Pérez-Morán[1], V Nava[1,3] and R Rodríguez-Arias[1,2]**

[1] Tecnalia Research & Innovation, Energy division, Offshore Renewable Energy area; Technology park of Bizkaia, Build. 700, Derio 48160, Basque Country, Spain
[2] Nautilus Floating Solutions S.L.; Technology park of Bizkaia, Build. 612, Derio 48160, Basque Country, Spain
[3] BCAM - Basque Centre for Applied Mathematics; Alameda Mazarredo 14, Bilbo 48009, Basque Country, Spain

josean.galvan@tecnalia.com

**Abstract**. This study presents two numerical multiphysics models of the *NAUTILUS-10* floating support structure mounting the *DTU10 MW Reference Wind Turbine* at Gulf of Maine site, and analyses its dynamics. With the site conditions and the FAST model of the onshore turbine as the starting point, the floating support structure: tower, floating substructure with its corresponding active ballast system and station keeping system, was designed by NAUTILUS. The numerical models were developed and the onshore *DTU wind energy controller* was tuned to avoid the resonance of the operating FOWT by TECNALIA, in the framework of H2020 LIFES50+ project. This concept and its subsystems are fully characterised throughout this paper and implemented in opensource code, FAST v8.16. Here, the mooring dynamics are solved using MoorDyn, and the hydrodynamic properties are computed using HydroDyn.Viscous effects, not captured by radiation-diffraction theory, are modelled using two different approaches: (1) through linear and quadratic additional hydrodynamic damping matrices and (2) by means of Morison elements. A set of simulations (such as, decay, wind only and broadband irregular waves tests) were carried out with system identification purposes and to analyse the differences between the two models presented. Then, a set of simulations in stochastic wind and waves were carried out to characterise the global response of the FOWT.

## 1. Introduction

The study summarises the state-of-the-art multiphysics numerical models of *NAUTILUS-DTU10* MW Floating Offshore Wind Turbine (FOWT) designed for Gulf of Maine (GoM) site, developed in the framework of the H2020 LIFES50+ project. A public repository [1] contains detailed description of these numerical models and the designer's technical report [2].

The FOWT is composed by the Rotor-Nacelle Assembly (RNA) of the *DTU 10 MW Reference Wind Turbine* (RWT) [3] and *NAUTILUS-10* floating support structure. The main innovation of NAUTILUS FOWT is the introduction of a Platform Trim System (PTS) which cancels /reduces the wind-induced mean trim angle by means of a variable sea water ballast system. This smart floating

structure is complemented with a tuned version of the onshore *DTU wind energy controller* [4] acting on the wind turbine.

Two numerical models are described, both implemented in FAST code [5], [6], using 8.16 version. While both numerical models have been developed to account for the active ballast dependent properties, the difference between these two models relays on the hydrodynamic modelling.

## 2. *NAUTILUS-DTU10* MW FOWT description

*NAUTILUS-DTU10* MW FOWT is composed by a 10 MW Horizontal Axis Wind Turbine (HAWT): *DTU 10 MW RWT* and the NAUTILUS support structure, designed for GoM site characteristics [7]. Inside this paper, the FOWT is divided in two main subsystems: (1) the RNA and (2) the support structure, being the latter composed by the tower, the floating substructure and the Station Keeping System (SKS).

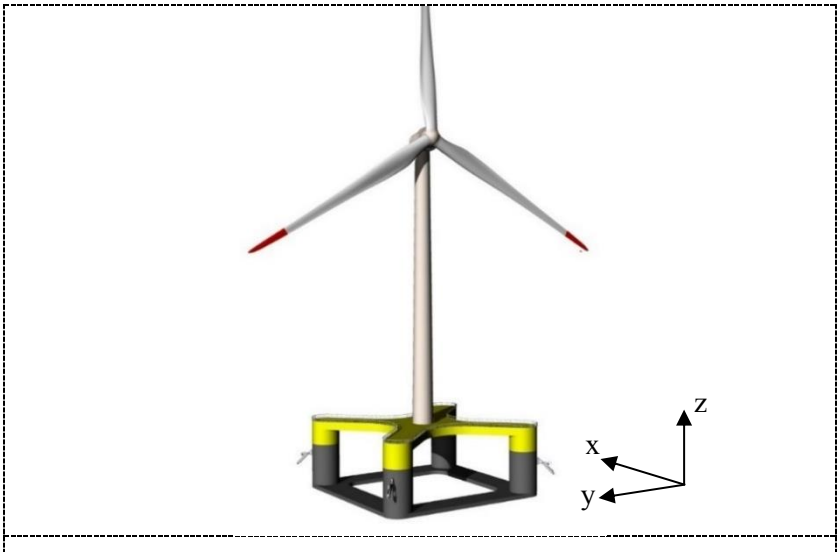


**Figure 1.** *NAUTILUS-DTU10* MW FOWT concept.

The *DTU 10 MW* RNA is mounted on the *NAUTILUS-10* floating substructure (Figure 1, being *NAUTILUS-DTU10* the complete FOWT system identification). The SKS designed consists of four standard catenary mooring lines anchored to the seabed of GoM. The whole system is controlled to behave smoothly by means of the wind turbine actuators and tuned WT controller, and the PTS to keep the tower vertical by flooding the tanks placed inside the columns with sea water ballast (WB) or pumping it outside the semisubmersible.

Following along this section, the properties of the FOWT and its subsystems/components are presented. This information is the basis for the development of the multiphysics numerical models.

### *2.1. FOWT properties*

As it has been briefly mentioned, *NAUTILUS-DTU10* presents variable weight distributions due to the PTS that controls the active ballast to cancel the FOWT heel/trim angle during energy production. The modification of the weights distribution inside the semisubmersible carries on the modification of the weight-dependant properties of the FOWT:

- Mechanical properties: mass, centre of mass (CM) and inertia
- Draft and draft-dependant variables: hydrostatic and hydrodynamic properties; location of the hub, tower base and fairleads.

*2.1.1. Mechanical properties.* The mechanical properties and displacement ($\rho_{SW} = 1{,}025$ kg/m$^3$) determined for the empty and fully loaded active ballast tanks are shown in Table 1, while the variation of these properties as function of wind speed at hub height and wind different directions can be found in [2].

**Table 1.** FOWT mechanical properties considering empty and fully loaded water tanks.

| **FOWT property** | Empty WB | Full WB | Units |
|---|---|---|---|
| Mass | 8,137,093 | 9,337,093 | [kg] |
| CM w.r.t. **k** CSys. | (-0.066 , 0 , 20.607) | (-0.058 , 0 , 20.113) | [m] |
| System roll / pitch / yaw radius of gyration | 47.19 / 47.22 / 26.50 | 45.61 / 45.64 / 28.40 | [m] |
| Operational draft w/ SKS | 14.952 | 18.333 | [m] |
| Displacement w/ SKS | 8,113.06 | 9,280.96 | [$m^3$] |

*2.1.2. Hydrostatic properties.* *NAUTILUS-DTU-10* MW FOWT, derived from this semisubmersible geometry, considering fully loaded WB tanks and including the SKS present a metacentric distance from keel (KM) of 34.623 m, while the centre of buoyancy is located 6.497 m above keel. Considering the FOWT CM (Table 1), the distance between CM and the metacentre (M) is then 14.881 m.

The hydrostatic stiffness terms for a floater draft of 18.333 m, horizontally positioned and without accounting for the mass restoring effects are: $C_{33} = 3.505 \cdot 10^6$ N/m, $C_{44} = 1.5373 \cdot 10^9$ N·m/rad and $C_{55} = 1.5513 \cdot 10^9$ N·m/rad.

*2.1.3. Hydrodynamic properties.* Due to the different approaches employed in the numerical hydrodynamic models presented in section 3, the hydrodynamic characterisation of the FOWT is presented in the mentioned section which describes both models.

*2.2. FOWT subsystems/components*

*2.2.1. DTU 10 MW RNA.* The *DTU 10 MW RWT* was designed and analysed inside LigthRotor danish project and INNWIND EU project by Vestas, DTU and the INNWIND Consortium [8]. The RNA of this wind turbine was selected as reference for the design of the floating support structures inside LIFES50+ project [9].

This RNA is designed for a wind regime IEC Class 1A and develops 10 MW of power at nominal above nominal wind speed (11.4 m/s). The three bladed upwind rotor has a diameter of 178.33 m and spins in the range from 6 to 9 rpm. Cut-in and cut-out wind speed are 4 m/s and 25 m/s, respectively. Further information about this RNA can be found in [3], [8], [9].

*2.2.2. DTU wind energy controller.* This controller was conceived for the *DTU 10 MW RWT* which is an onshore WT. The controller is inspired on previous DTU controllers and the modifications proposed in [10] for the *NREL 5 MW WT* controller inside UpWind EU project.

**Table 2.** Tuned WT controller parameters in the full load region.

| | Value | Units |
|---|---|---|
| Proportional gain of pitch controller | 0.208004 | [rad/(rad/s)] |
| Integral gain of pitch controller | 0.041415 | [rad/rad] |
| Differential gain of pitch controller | 0.0 | [rad/(rad/$s^2$)] |
| Proportional power error gain | $0.4 \cdot 10^{-8}$ | [rad/W] |
| Integral power error gain | $0.4 \cdot 10^{-8}$ | [rad/(W·s)] |
| Linear coeff. in aerodynamic gain scheduling, KK1 | 5.498310 | [deg] |
| Quadratic coeff. in aerodynamic gain scheduling, KK2 | 386.005941 | [$deg^2$] |
| Relative speed for double nonlinear gain | 1.3 | [-] |

The control strategies implemented in the *DTU wind energy controller* are based on the traditional onshore HAWT controllers which consider two main operating regions: (1) partial load region and (2) full load region, where the blade pitch controller acts with the main objective to maintain a constant power or torque, depending on the strategy selected.

The controller setup in the partial load region remains unmodified. In the full load region, by contrast, the controller strategy objective has been switched from a constant power output to a constant torque; and to avoid the negative damping induced motion amplifications, the controller parameters have been tuned (Table 2).

*2.2.3. NAUTILUS-10 tower.* At earliest stage of the design, the original onshore tower of the *DTU 10 MW RWT* was analysed installed on the moored semisubmersible. As it was expected, that onshore design falled inside the rotor 3P excitation due to the stiffness reduction of the floating substructure compared to rigid ground; therefore *NAUTILUS-10* tower was conceived to dynamically behave as a stiff/stiff tower once installed in the FOWT.

It is a conical single piece tower design of linearly varying thickness. The tower base is connected to the floating substructure by a transition piece at tower-platform interface. This component is embedded into the main deck of the floating platform and thus, it is considered part of the hull. The tower base presents an outer diameter of 10.5 m, meanwhile the tower top conserves the 5.5 m outer diameter to fulfil RNA requirements [3]. Tower base and top thickness are 0.040 m and 0.037 m, respectively. The tower has a total length of 107 m. once the FOWT is installed and considering the fully filled ballast tanks, the tower base is located 7.667 m above MSL. Note that this distance will vary with the WB levels in the tanks.

The tower is made of steel S-355-J2H. Material density has been augmented to 8,500 kg/m$^3$ to account for the mass of "realistic" tower sections flanges, secondary structures, etc., as it was done in other public WT tower models [11]. The total tower mass is 879,381 kg and its CM is located 47.241 m above tower base. Distributed mechanical and structural properties of the tower can be found in [2].

*NAUTILUS-10* tower installed onshore and on the free-floating and moored floater, supporting the RNA mass presents the natural frequencies shown in Table 3. These results have been obtained resolving the eigenproblem of the undamped system where the RNA is modelled as a point mass.

**Table 3.** *NAUTILUS-10* tower undamped natural frequencies considering different boundary conditions and 1,200 tonnes of WB.

| **Modeshape** | Onshore | Free-floating | Moored | Units |
|---|---|---|---|---|
| 1$^{st}$ Side-to-Side | 0.3930 | 0.5435 | 0.5407 | [Hz] |
| 1$^{st}$ Fore-Aft | 0.3970 | 0.5508 | 0.5478 | [Hz] |
| 1$^{st}$ Twist | 1.5125 | 1.5180 | 1.5179 | [Hz] |
| 2$^{nd}$ Side-to-Side (coupled with 2$^{nd}$ twist) | 1.9493 | 2.0058 | 2.0042 | [Hz] |
| 2$^{nd}$ Fore-Aft | 2.2372 | 2.2979 | 2.2962 | [Hz] |

As it can be seen the first Fore-Aft (FA) and Side-to-Side (SS) natural frequencies of the tower for the moored configuration are between the rotor 3P and 6P frequencies, corresponding to a stiff-stiff tower design.

*2.2.4. NAUTILUS-10 floating substructure. NAUTILUS-10* semisubmersible type platform is an upscaled (and modified) version of the concept developed for the *NREL 5 MW WT [12]* by TECNALIA for NAUTILUS Floating Solutions S.L. The main modifications that are relevant for this study are: (1) the central heave-plate is removed and (2) the column height $h_C$, and therefore the freeboard, has been reduced.

NAUTILUS is a symmetric semisubmersible floating platform (Figure 1), whose **hull** is composed by four columns connected at keel plane by a square-shaped ring pontoon and by an X-shaped main

deck at columns top. The transition piece to connect the tower is embedded in the main deck centre. All the structure is compartmented to keep the structure water tight. The structure is made of structural steel S-275 J2 and S355. The conceptual design of *NAUTILUS-10* semisubmersible to support *DTU 10 MW* RNA installed on the described tower at Gulf of Maine site, presents the dimensions and operational draft shown in Table 4.

**Table 4.** Geometrical properties of *NAUTILUS-10* concept components and floater draft.

| ***NAUTILUS-10* design variable** | Value | Units |
|---|---|---|
| Transition piece height, $h_{TP}$ | 3.00 | [kg] |
| Transition piece diameter, $d_{TP}$ | 10.50 | [m] |
| Main deck width, $w_{MD}$ | 10.50 | [kg·m$^2$] |
| Main deck height, $h_{MD}$ | 3.00 | [kg·m$^2$] |
| Distance between columns, $L_C$ | 54.75 | [kg·m$^2$] |
| Column diameter, $d_C$ | 10.50 | [m] |
| Column height, $h_C$ (from keel to deck top) | 26.00 | [m] |
| Pontoon width, $w_P$ | 10.50 | [m] |
| Pontoon height, $h_P$ | 1.50 | [m] |
| Equilibrium draft (including RNA, tower and SKS) | 18.33 | [m] |

FOWT stability is increased by means of ballasting the ring pontoon with 3,885 tonnes of concrete. The concrete ballast (CB) reaches a height of 0.71 m w.r.t. to the keel line of the floater.

The columns, which are compartmented above pontoon height, store movable seawater ballast (WB) in the lowest compartment with up to 300 tonnes of active ballast per column. This removable seawater ballast mass is modified under control of the Platform Trim System (PTS).

Following, the mechanical properties of *NAUTILUS-10* semisubmersible considering hull, passive ballast mass and (1) empty and (2) full loaded seawater ballast tanks are shown in Table 5. Further information about the mechanical properties of *NAUTILUS-10* can be found in [2].

**Table 5.** Mechanical properties of the semisubmersible including CB and considering empty and fully loaded WB tanks.

| **Floating substructure property** | Empty WB | Full WB | Units |
|---|---|---|---|
| Mass | 6,581,000 | 7,781,337 | [kg] |
| CM w.r.t. **k** CSys. | (0 , 0 , 4.204) | (0 , 0 , 4.050) | [m] |
| System roll / pitch / yaw radius of gyration | 24.41 / 24.41 / 29.26 | 24.91 / 24.91 / 30.95 | [m] |

As it can be derived from this table, the WB increases the floater roll and pitch inertia in 23% and 32% in the case of yaw one, which effectively is translated in higher periods. The platform mass, by its side, is increased in 18% and a slightly reduction (<4%) of the vertical position of the CM is also achieved when the full WB mass (1,200 tonnes) is considered.

*2.2.5. NAUTILUS-10 Platform Trim System. NAUTILUS-DTU10* MW FOWT cancels/reduces the mean wind-induced trimming and heeling by means of a Platform Trim System (PTS), thus restoring the platform to an optimal position (vertical tower) from the WT performance point of view.

The PTS has three sensors that are responsible of measuring the FOWT roll and pitch amplitude and the draft.

The control system actuator is the pumping system. Opposite to other active ballast systems oriented to floating wind turbines which do not modify the draft [13], [14]; this system pumps sea

water independently into/out to each of the individual columns. The controller acts on the valves opening and water pumps to vary the WB level. Up to 300 tonnes of sea water ballast could be taken off in approximately 30 min using two independent flow paths with redundant pumping capability.

As it can be glimpsed, when the WT is operating, the WB distribution will be driven by FOWT mean heel/trim amplitudes which are tightly related to thrust force magnitude and direction which at the same time depends on the next parameters:

- Wind speed.
- Effective wind direction, which depends on the mean wind flow direction and the nacelle yaw.

Although the sea state (SS) also influences the FOWT rotational displacements, its contribution to the total mean amplitude has been found to be minimal when the WT is operating around rated wind speed. Thus, for *NAUTILUS-DTU10* MW FOWT the PTS has been simplified to a wind speed dependant WB distribution. Considering the wind aligned with global X-axis, the WB mass in the upwind columns tanks will be constant (300 tons) and the downwind tanks will pump out WB (300 tonnes present for 0 m/s wind speed) until the FOWT heel angle is cancelled (see Figure 2 and [2] for further information).

Due to the variable draft characteristic of *NAUTILUS-10* floating support structure, the hub height above the mean sea level (MSL) will vary according to the WB distribution (Figure 2).

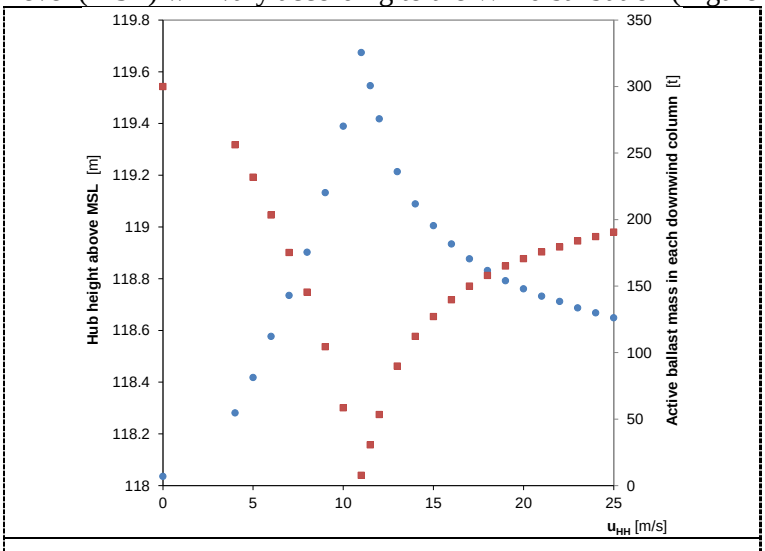


**Figure 2.** Hub height (blue) as function of wind speed due to water ballast (red) variation in downwind tanks.

Some additional advantages of installing a PTS in a FOWT are pointed below:

- More flexibility to vary draft which could prevent from wave slamming over the deck under non-operational extreme conditions. Regarding inspection and maintenance, the control over draft can simplify these two tasks on the floating platform.
- Under damaged condition (i.e., due to a collision), the floating platform disposes of additional resources to pump out the sea water.

*2.2.6. NAUTILUS-10 station keeping system.* The aim of the SKS is to avoid the FOWT from drifting and therefore to maintain the power cable within a sufficient stress range. For this purpose, the floater is moored with four catenary lines (Figure 1).

Gulf of Maine seabed presents 4 m of dense sand [7] which enables the use of conventional drag anchors to keep lines secured to seabed. The design water depth was set to 130 m for LIFES50+ EU project, meanwhile water density of 1,025 kg/m$^3$ was considered. The seabed is assumed to be horizontal and flat.

Fairleads are located 12 m above the floater's keel line which let them 6.333 m below MSL when the FOWT is in its undisplaced position (draft of 18.333 m), and 43.96 m, in XY-plane, from platform

centreline. Drag anchors are fixed to seabed at 793.50 m from fairlead position and therefore to 837.46 m from *NAUTILUS-10* centreline. All mooring lines have the same unstretched length of 833.24 m.

The mooring lines selected are studless chains of 97 mm of bar nominal diameter. The chain distributed mass is 188.16 kg/m and the extensional (axial) stiffness is 803.5 MN. The SKS pretension derived from this layout is then 406,300 N.

## 3. Multiphysics modelling of *NAUTILUS-DTU10* MW FOWT

This section is fully dedicated to the description of the numerical multiphysics models that have been implemented to capture the FOWT aero-hydro-servo-elastic behaviour through time domain coupled simulations. FAST 8.16 32-bit version code [15] has been employed to build these models. Following, this section is structured according to the physics that are part of the problem.

### *3.1. Multibody dynamics*

FAST v8.16 presents a modular framework which is articulated around the multibody dynamics model that represents the FOWT. This model is the responsible of solving the nonlinear equations of motion of the system and of feeding with the calculated displacements, velocities and accelerations the multiphysics modules that determine the loads to be applied to the multibody model. The multibody formulation is combined with a modal superposition approach to represent the flexible elements of the FOWT (blades and tower). The FOWT model implemented accounts for a total of 23 DOFs.

### *3.2. Elastodynamics*

The drivetrain, blades and tower of the FOWT are considered flexible inside the models presented here. While the drivetrain is represented by a single degree of freedom (DOF) representing its torsion, the tower and each blade consider 4 and 3 DOFs, respectively. The tower modeshapes included in the modal superposition approach implemented in ElastoDyn are: the 1$^{st}$ and 2$^{nd}$ fore-aft and side-to-side. The tower is meshed with a total of 30 equally spaced nodes.

Taking into account the geometry, the structural and aerodynamic properties of the prebended blade of *DTU 10 MW RWT* [3], a high fidelity model like that implemented in BeamDyn [16], [17] would be advisable. Nevertheless, the blade model distributed inside the LIFES50+ project was simplified to a straight blade model [9]. This simplification was considered to overcome the numerical efficiency problems detected in BeamDyn of FAST v8.12, initially employed in LIFES50+ project.

Then, the blade model considered here accounts for 1$^{st}$ and 2$^{nd}$ flapwise modeshapes and considers just the 1$^{st}$ edgewise. A total of 50 structural elements are used in the discretisation of this component.

### *3.3. Aerodynamics*

As in the case of elastodynamics, the blade properties have been adapted, so the rotor shows very similar aeroelastic performance when using the high fidelity or the modal superposition approach to calculate elastodynamics. The blade aerodynamic mesh defined in [9] is composed by 37 nodes.

Rotor aerodynamics have been modelled using an engineering-level model based on the modified Blade Element Momentum theory that AeroDyn v14.05 implements [18]–[20]. Note that nor the tower influence on the flow around the blade nor the wind loading on the tower and floater have been considered in the results presented in this paper. The reason for this important simplification is that the *DTU 10 MW RWT* aerodynamics have not been defined for AeroDyn v15 code [9], the first release including these capabilities in the analysis of floating support structures [21].

### *3.4. Servodynamics*

*3.4.1. WT controller.* This controller is distributed under a 32 bit Dynamic Library Link (DLL) package, in the style of Garrad Hassan's BLADED WT software which can communicate with ServoDyn module of FAST [22]. These files and the tuned input files can be download from [1].

*3.4.2. Platform trim system.* On the other hand, the floating platform control system dynamics are not considered along the coupled dynamic simulations due to its large response period (as in the case of nacelle yaw controller for onshore WTs). The sea water ballast distribution is determined prior to the simulation and it remains constant along all the simulation.

Although the inclusion of the dynamics of PTS opens the study to combined strategies between the WT and floater's controllers, this topic will not be covered in the present paper.

*3.5. Hydrodynamics*

As result of the comparison of the hydrodynamic loads due to two different sea states (NSS and ESS) in [2], it was concluded that for the case of *NAUTILUS-DTU10* MW FOWT the Potential Flow (PF) solution obtains satisfactory results under NSS, but by contrast under ESS, the viscous effects should not be neglected. Same conclusions were obtained in [23] for the OC4 DeepCwind semisubmersible.

Following the previous recommendations, two hydrodynamics models have been implemented in HydroDyn for comparison purposes, identified as PF+AHD (potential flow + additional hydrodynamic damping) and PF+ME (potential flow + Morison elements), differing on the modelling of turbulent effects. While additional hydrodynamics models in [2] are based on a variable submerged volume, both numerical hydrodynamics models presented here consider a constant submerged volume.

*3.5.1. Hydrodynamics: Potential flow solution.* For the studied geometry, calculations have been carried out using a higher order panel method with the maximum panel size considered is 2 m, with a frequency resolution of 0.02 rad/s, considering no RNA eccentricity, under fully loaded WB condition and hull keel plane horizontal due to PTS.

For the calculation of the mean drift force, FOWT mechanical properties (Table 1) and the linearized mooring stiffness matrix $K_M$ is also given to the solver, while no additional damping was included at this stage (due to the absence of reliable damping values), provided that results were considered acceptable.

*3.5.2. Hydrodynamics: Viscosity through additional hydrodynamic damping vs Morison elements.* In the PF+AHD model, AHD values (Table 6) were determined through an upscaling process of *NAUTILUS-NREL5* MW concept, which had been experimentally tested at two different scales [12], [25], asdescribed in [2].

**Table 6.** Linear and quadratic AHD values of *NAUTILUS-DTU10* MW FOWT.

| | Linear AHD terms | | Quadratic AHD terms | |
|---|---|---|---|---|
| **DOF** | Value | Units | Value | Units |
| Surge | 0 | [N·s/m] | 1,100,985 | [N·s$^2$/m$^2$] |
| Sway | 0 | [N·s/m] | 827,308 | [N·s$^2$/m$^2$] |
| Heave | 335,479 | [N·s/m] | 5,637,998 | [N·s$^2$/m$^2$] |
| Roll | 211.97·10$^6$ | [N·m·s/rad] | 38,515.2·10$^6$ | [N·m·s$^2$/rad$^2$] |
| Pitch | 222.17·10$^6$ | [N·m·s/rad] | 41,617.9·10$^6$ | [N·m·s$^2$/rad$^2$] |
| Yaw | 22.56·10$^6$ | [N·m·s/rad] | 7,066.5·10$^6$ | [N·m·s$^2$/rad$^2$] |

The drag terms of Morison's equation (ME) can be computed by combination with the strip theory. The mesh defined to calculate the submerged volume and described in [2] is used here.

Table 7 collects the drag coefficients and dimensions of the members that the platform has been decomposed into. These values have been fitted to account for the inter-member interactions and show a hydrodynamic behaviour comparable to that obtained with the PF+AHD model, which accounts for the interaction between the submerged members under waves (but not current) conditions.

**Table 7.** Morison elements and drag coefficients of *NAUTILUS-10* semisubmersible. *$C_{D,a}$ is only applied at the lower end of the member.

| | Modelling geometry | | Drag coefficients | |
|---|---|---|---|---|
| **Member** | $d$ [m] | $L$ [m] | $C_{D,a}$* [-] | $C_{D,t}$ [-] |
| Pontoon(s) | 4.478 | 44.250 | - | 2.0000 |
| Ring pontoon rounded corner(s) | 4.617 | 1.500 | 1.0483 | - |
| Column(s) connection w/ pontoons | 4.753 | 1.500 | - | - |
| Column(s) | 10.500 | 26.000 | 0.8745 | 0.9600 |
| Virtual column | 6.529 | 1.500 | 550.0000 | - |

### *3.6. Mooring dynamics*

Meanwhile in [2] up to four different mooring dynamics codes (MAP++, MoorDyn, FEAM and OrcaFlex) are analysed and compared in time domain, coupled and decoupled from the overall multiphysics problem. Here, the SKS dynamics will be resolved using MoorDyn code [26]. The mooring line properties are determined from OrcaFlex [27] database and adapted to the theory behind MoorDyn, as shown in Table 8 where the difference between both codes can be derived.

**Table 8.** Mooring lines properties considered in the numerical codes.

| | MoorDyn | OrcaFlex | Units |
|---|---|---|---|
| Hydrodynamic diameter in normal direction | 0.097 | 0.097 | [m] |
| Hydrodynamic diameter in axial direction | 0.097 | 0.031 | [m] |
| Diameter for line-to-seabed friction | - | 0.302 | [m] |
| Drag coefficient in normal direction, $C_{D,N}$ | 2.400 | 2.400 | [-] |
| Drag coefficient in axial direction, $C_{D,Axial}$ | 0.368 | 1.15 | [-] |
| Drag coefficient in normal direction, $C_{A,N}$ | 1.000 | 1.000 | [-] |
| Added mass coefficient in axial direction, $C_{A,Axial}$ | 0.160 | 0.500 | [-] |
| Line-to-seabed friction coefficient, $C_{D,N}$ | - | 0.0 | [-] |
| Structural damping ratio, $\xi_{Line}$ | 1.0 | 1.0 | [%] |

## 4. Tests and Design Driving Load Cases: Definition and results

### *4.1. Decay tests*

These tests dedicated to identifying the system properties are performed in calm water without and with the presence of uniform wind (4, 8, 11.4, 18 and 44 m/s) parallel to global X-axis (Figure 1). This set of tests provide the designers wide information about eigenfrequencies of the platform, linear and quadratic damping and linearity effects. The considered initial offsets from equilibrium position are 10 m, 2 m and 8 degrees for surge, heave and pitch, respectively.

The free decay tests without wind (Figure 3, top) reveal that a very good match between the hydrodynamic models proposed is achieved, finding slight differences in the first cycles of surge test.

When steady wind is present and the rotor is operating, there are three main factors that will modify the floater periods: (1) the SKS stiffness at equilibrium, (2) rotor introduced aerodynamic damping and (3) the PTS driven WB distribution to adapt to wind characteristics. The variation of the periods due to SKS stiffness can be clearly observed in surge decay tests; because of the lower contribution

this parameter to heave and pitch motion (for the case of this semisubmersible), the variation of the periods due to mass variation and aerodynamic damping are more noticeable in heave and pitch tests.

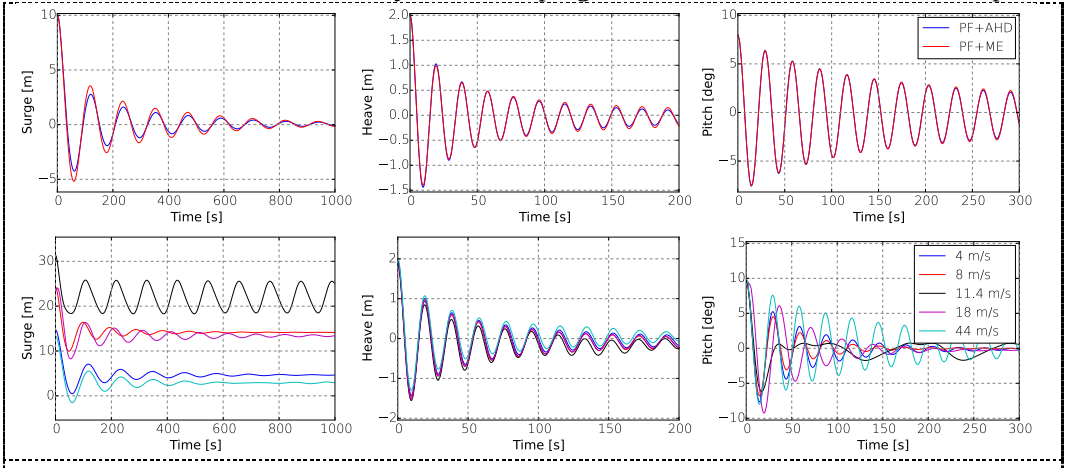


**Figure 3.** Decay tests of *NAUTILUS-DTU10* FOWT w/o wind (top, comparison of hydrodynamic models) and operating w/ steady wind (bottom, PF+AHD).

As it can be seen in Figure 3, surge and pitch tests operating at nominal wind speed do not completely decay and some resonance phenomena can be observed in surge motion. This resonance is mainly due to the WT controller setup, which was tuned considering a stepped wind case without ocean loading (section 4.3) showing a stable behaviour. It should be noted that this self-excitation reduces/disappears when irregular waves are present, due to the randomness of the excitation frequency. Nominal wind in still water in not a load case (LC) expected in GoM. The reproduction of this instability is very sensitive to the initial blades pitch condition.

### *4.2. Wind tests*

Uniform wind type with increasing speed (1 m/s steps of 300 s) confined between the rotor cut-in to cut-out limits is considered here to assess the FOWT dynamics behaviour under operation. To ensure the dynamic stability of the system, the inclusion of waves is neglected and thus, significant values of hydrodynamic damping too. Additionally, the response has been calculated for WB distributions that correspond to 4 and 11.4 m/s wind speed.

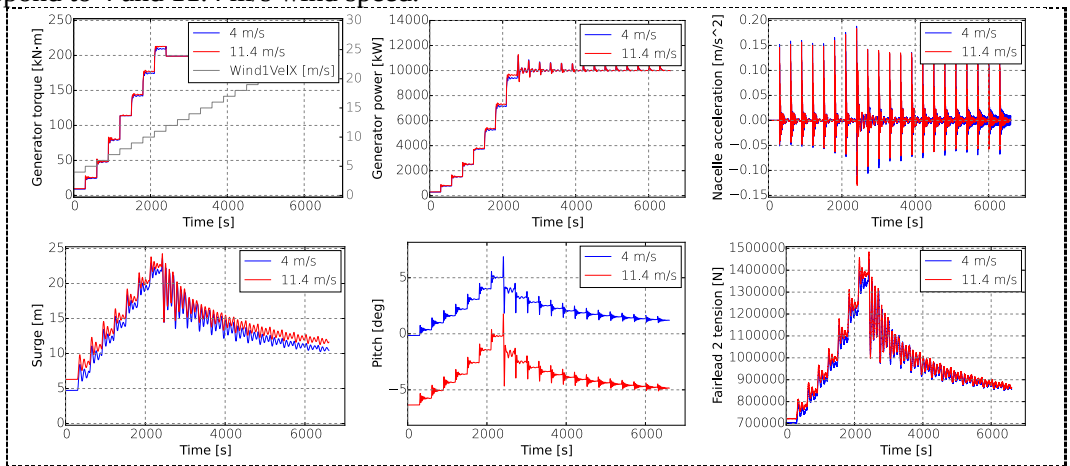


**Figure 4.** FOWT performance under stepped wind.

In the case of FOWTs the wind range affecting the full-load region of the controller is of special interest (rotor thrust decreasing region). The constant torque strategy is clearly shown in Figure 4. The controller tuning will also depend on the maximum allowable generated power, which already is unknown. Nacelle accelerations show a slightly lower maximum and more stable response under the

11.4 m/s WB distribution. Non-zero mean pitch offsets indicate a suboptimal setup and /or distribution of the ballast, fact visible through the wind speed ranges different to that considered (4 m/s and 11.4 m/s) at the beginning of the simulation. This effect is partially induced by the static character of the simulation, but it should be noticed that the response time of the proposed PTS (≈0.15 deg/min) will be able to answer to such speed steps that are maintained constant during 5 min. The relation between surge motion and fairlead tension can be observed in the results above.

### *4.3. Broadband irregular waves tests*

Broadband spectrum waves tests are very useful to characterise the hydrodynamic behaviour as the system is excited in a wide range of frequencies. The energy of the waves is distributed here in a white noise pattern from 4.5 to 18.2 s for two different wave heights (2 and 4 m) and headings (-15 and 90 deg) considering two hours simulation length (excluding transients).

The results are presented in Figure 5 under the form of power spectral density (PSD) of the most relevant DOFs of the floater. No significant differences can be observed in the low frequency translations (surge and sway) independently from wave height. PF+ME calculates a more damped yaw response, opposite to heave motion where larger energy content is present at heave natural frequency. Both models obtain nearly identical roll and pitch response, independently of wave height.

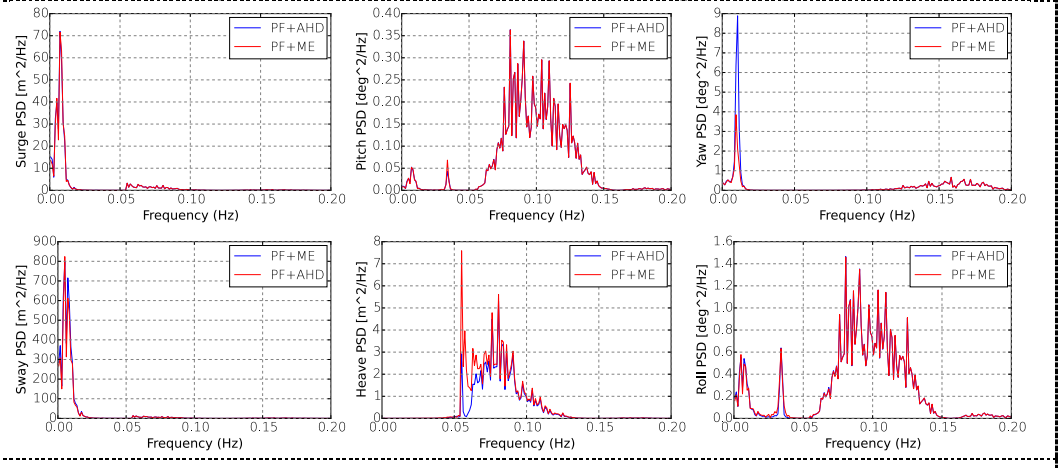


**Figure 5.** Comparison of the hydrodynamic models under white noise tests. $H_S = 2$ m, $\alpha_{Wave} = -15$ deg (top) and $H_S = 4$ m, $\alpha_{Wave} = 90$ deg (bottom).

### *4.4. Design driving load cases: Turbulent wind and irregular waves at Gulf of Maine*

Finally, closing the analysis section of this paper, the spectrum-compatible irregular waves and turbulent wind expected at Gulf of Maine are analysed. A reduced set of Design Load Cases (DLCs), coherent with IEC standards, has been selected for this paper (Table 9), which indeed are part of the *NAUTILUS-DTU10* MW FOWT Design Driving Load Cases (DDLCs) set.

**Table 9.** Turbulent wind ($\alpha_{Wind} = -15$ deg) and irregular waves DLCs.

| **DLC Id.** | $U_{HH}$ [m/s] | $I_{Turb}$ [%] | Shear [-] | Wave direction [deg] | $H_S$ [m] | $T_P$ [s] |
|---|---|---|---|---|---|---|
| DLC 1.6_1/2/6 | 8.0/11.4/18.0 | 8.3/8.4/8.7 | 0.14 | -15 | 7.7/7.7/10.9 | 12.4/12.4/15.0 |
| DLC 1.6_7 | 11.4 | 8.4 | 0.14 | 90 | 7.7 | 12.4 |
| DLC 5.1 | 11.4 | 12.8 | 0.14 | 0 | 1.6 | 25 |
| DLC 6.1_2a | 44.0 | 11.0 | 0.11 | -15 | 10.9 | 15.0 |

A fault condition DLC has been included: DLC 5.1. This LC considers the loss of the electrical grid while operating at rated wind speed and thus, a rapid reduction of the mechanical torque (and

thrust consequently) will occur to due to blade pitching to avoid rotor over-acceleration. This is a DDLCs for the *NAUTILUS-10* PTS and the unphysical wave of 25 s period has been chosen to excitate heave and roll/pitch motion. This DLCS should be taken into consideration in all the actively ballasted floating substructures; as the WB distribution for this wind condition will augment the maximum pitch amplitude generated during the transients.

The maximum pitch rotation remains above -15 degrees after the loss of grid (Figure 6) and the response decays until equilibrium. Due to the reduction of thrust, FOWT excursion is reduced while the nacelle accelerations induced by the transients remains below 0.6 m/s$^2$.

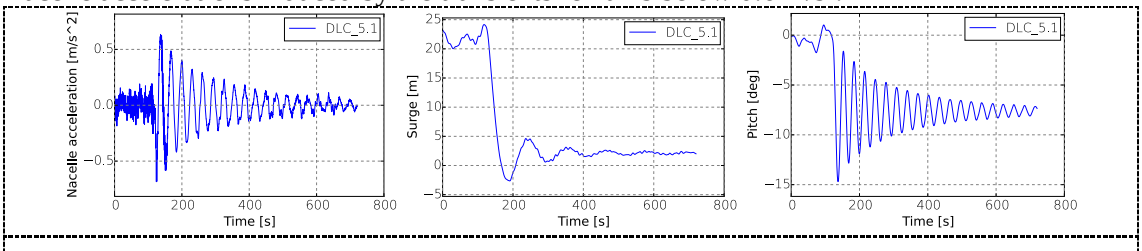


**Figure 6.** FOWT response operating at nominal wind speed and with loss of grid.

Some key parameters of the FOWT behaviour determined from the DLCs dedicated to study ULS are summarised below (Table 10). The results, calculated employing PF+AHD model, are presented in terms of their statistical mean and standard deviation. It can be observed that power production under SSS (DLC 1.6_X) is the most exigent and achieves larger mean values and standard deviations.

**Table 10.** Statistics of *NAUTILUS-DTU10* MW FOWT key parameters.

| | DLC 1.6_X | | | DLC 6.1_2a | | | |
|---|---|---|---|---|---|---|---|
| **Output parameter** | Max | Mean | STD | Max | Mean | STD | Units |
| Generator power | 11,860 | 9,996 | 882 | - | - | - | [kW] |
| Blade root My | 37,670 | 25,324 | 4,630 | 5,821 | 868 | 1,585 | [kN·m] |
| Combined RNA acceleration | 1.99 | 0.40 | 0.22 | 1.51 | 0.41 | 0.20 | [m/s$^2$] |
| Combined tower base moment | 329,892 | 138,956 | 59,300 | 183,367 | 51,446 | 26,282 | [kN·m] |
| Floater excursion | 27.92 | 21.50 | 2.87 | 10.49 | 5.52 | 1.68 | [m] |
| Combined floater heel/trim | 6.90 | 1.44 | 0.99 | 3.02 | 0.91 | 0.45 | [deg] |
| Mooring line tension | 2,511 | 1,558 | 213 | 1,025 | 741 | 69 | [kN] |

## 5. Conclusions

The inclusion of the active ballast control system in *NAUTILUS-10* semisubmersible brings some challenges to the numerical modelling of this concept. While most of these challenges increase the time during the FOWT design and validation processes, some simplifications that can be applied to this concept to reduce the demand of these resources have also been mentioned.

To validate the concept against a reduced set of DDLCs, two numerical models have been presented. When both are applicable, PF+AHD is 30% faster than PF+ME model, which is particularly convenient during the first design loops of the concept. Nevertheless, when implemented thorugh FAST's HydroDyn module, PF+AHD cannot model the current induced loading/damping.

The numerical results show that controller dynamics and hydrodynamic loading/damping play an important role in the dynamic stability of the FOWT and demonstrate the satisfactory behaviour of *NAUTILUS-DTU10* MW Floating Offshore Wind Turbine.

After the first design iteration presented here, future work will focus on the WT controller and communication with the PTS and the calibration of the hydrodynamic models against experimental tests. The inclusion of the submodels to capture tower and floater aerodynamics will be of special interest too, linked to the development of the BeamDyn model of the blades.

In order to make this information public to the research community and support the development of Floating Offshore Wind technology, the FOWT designer's information and the numerical models developed and presented here can be found at: https://www.researchgate.net/project/NAUTILUS-DTU10-MW-Floating-Offshore-Wind-Turbine-at-Gulf-of-Maine.

**Acknowledgments**
The research leading to these results has received funding from the European Union Horizon2020 programme under the agreement H2020-LCE-2014-1-640741, LIFES50+ project.

**References**

[1] Tecnalia R&I; Offshore Renewable Energy area, 'The NAUTILUS-DTU10 MW Floating Offshore Wind Turbine Project site', 03-Apr-2018. [Online]. Available: https://www.researchgate.net/project/NAUTILUS-DTU10-MW-Floating-Offshore-Wind-Turbine-at-Gulf-of-Maine. [Accessed: 04-Apr-2018].
[2] J. Galvan *et al.*, 'Definition and Analysis of NAUTILUS-DTU10 MW Floating Offshore Wind Turbine at Gulf of Maine: Experiments at Sintef Ocean & PoliMi', Tecnalia R&I, Derio, Basque Country, Spain, Public use under permission TRI-ORE-PUB-001\2017, Dec. 2017.
[3] C. Bak *et al.*, 'Description of the DTU 10 MW reference wind turbine', DTU Wind Energy, DTU Wind Energy Frederiksborgvej 399 4000 Roskilde, Denmark, I–0092, Jul. 2013.
[4] M. H. Hansen and L. C. Henriksen, 'Basic DTU Wind Energy controller', DTU, Department of Wind Energy, DTU, Denmark, E-0028, Jan. 2013.
[5] B. Jonkman and J. Jonkman, 'Readme file for FAST v8.16.00a-bjj', 26-Jul-2016. [Online]. Available: https://wind.nrel.gov/nwtc/docs/README_FAST8.pdf. [Accessed: 16-Oct-2014].
[6] J. M. Jonkman and M. L. Buhl Jr, *FAST user's guide*. Golden, CO, USA: National Renewable Energy Laboratory, 2005.
[7] A. Krieger, G. K. V. Ramachandran, L. Vita, P. Gómez Alonso, J. Berque, and G. Aguirre, 'D7.2 Design basis', DNV GL; IBERDROLA Ingeniería y Construcción; Tecnalia R&I, Public LIFES50+ D7.2, Nov. 2015.
[8] P.K. Chaviaropoulos, D. Chortis, and D. Lekou, 'Definition of the reference Wind Turbine - Analysis of Rotor Design Parameters', CRES, Public INNWIND D1.2.1, May 3013.
[9] M. Borg, M. Mirzaei, and H. Brendmose, 'D1.2 Wind turbine models for the design', DTU, Public LIFES50+ D1.2, Dec. 2015.
[10] E. Bossanyi, 'Controller for 5 MW reference turbine', Garrad Hassan & Partners Limited, UpWind report 11593/BR/04, Jul. 2009.
[11] J. Jonkman, S. Butterfield, W. Musial, and G. Scott, 'Definition of a 5-MW reference wind turbine for offshore system development', National Renewable Energy Laboratory, Golden, Colorado, U.S.A., NREL/TP-500-38060, 2009.
[12] Nava, V., Aguirre, G., Galvan, J., Sanchez-Lara, M., Mendikoa, I., and Perez-Moran, G., 'Experimental studies on the hydrodynamic behavior of a semi-submersible offshore wind platform', in *Proceedings of 1st International Conference on Renewable Energies Offshore*, Lisbon, Portugal, 2014, p. 7.
[13] I. Couchman and R. Bowyer, 'Coordinated control of a floating wind turbine', US 2015/0147174 A1, 28-May-2015.
[14] D. Roddier and C. Cermelli, 'Floating Wind Turbine platform with ballast control and mooring system', US 9,139,266 B2, 22-Sep-2015.
[15] NREL, 'FAST v8 | NWTC Information Portal', *NREL: NWTC Information Portal*, Jul-2016. [Online]. Available: https://nwtc.nrel.gov/FAST8. [Accessed: 29-Nov-2016].

[16] Q. Wang, M. Sprague, J. Jonkman, and N. Johnson, 'BeamDyn: A high-fidelity wind turbine blade solver in the FAST modular framework', presented at the SciTech 2015, Florida, USA, 2015.
[17] *BeamDyn User's Guide*. National Renewable Energy Laboratory Golden, CO, 2015.
[18] D.J. Laino and A.C. Hansen, *AeroDyn user's guide, version 12.50*. 2002.
[19] P. J. Moriarty and A. C. Hansen, *AeroDyn theory manual*. National Renewable Energy Laboratory Golden, Colorado, USA, 2005.
[20] B. Jonkman, *Using the NewTower feature of AeroDyn 14*. NREL.
[21] J. Jonkman, G.J. Hayman, B. Jonkman, and R.R. Damiani, *AeroDyn v15 user's guide and theory manual*. 2015.
[22] J. Jonkman, 'Overview of the ServoDyn control & electrical-drive module', presented at the NREL Wind turbine modelling workshop, Bergen, Norway, 11-Sep-2014.
[23] A. Robertson *et al.*, 'Offshore Code Comparison Collaboration Continuation within IEA Wind Task 30: Phase II results regarding a floating semisubmersible wind system', in *ASME 2014 33rd International Conference on Ocean, Offshore and Arctic Engineering*, 2014, p. V09BT09A012–V09BT09A012.
[24] K. Müller, R. Faerron-Guzmán, M. Borg, and A. Manjock, 'D7.7 Identification of critical environmental conditions and design load cases', STUTT, Public D7.7, Jul. 2018.
[25] V. Ayllon *et al.*, 'Análisis experimental de una plataforma flotante para la extracción de energía eólica en aguas profundas', IHC - Instituto de Hidráulica ambiental de la universidad de Cantabria, Cantabria, Memoria final de ensayos, Nov. 2014.
[26] M. Hall, *MoorDyn User's Guide*. University of Maine, 2014.
[27] Orcina Ltd., *OrcaFlex 10 user manual*. Orcina Ltd., 2016.